arXiv:astro-ph/0604536v1 26 Apr 2006

draft of February 5, 2008

Effects of Rotation on Thermal-Gravitational Instability in the Protogalactic Disk Environment

Chang Hyun Baek[1,2], Dongsu Ryu[3], Hyesung Kang[4], and Jongsoo Kim[2]

ABSTRACT

Thermal-gravitational instability (TGI) is studied in the protogalactic environment. We extend our previous work, where we found that dense clumps first form out of hot background gas by thermal instability and later a small fraction of them grow to virialized clouds of mass $M_c \gtrsim 6 \times 10^6$ $M_\odot$ by gravitational infall and merging. But these clouds have large angular momentum, so they would be difficult, if not impossible, to further evolve into globular clusters. In this paper, through three-dimensional hydrodynamic simulations in a uniformly rotating frame, we explore if the Coriolis force due to rotation in protogalactic disk regions can hinder binary merging and reduce angular momentum of the clouds formed. With rotation comparable to the Galactic rotation at the Solar circle, the Coriolis force is smaller than the pressure force during the early thermal instability stage. So the properties of clumps formed by thermal instability are not affected noticeably by rotation, except increased angular momentum. However, during later stage the Coriolis force becomes dominant over the gravity, and hence the further growth to gravitationally bound clouds by gravitational infall and merging is prohibited. Our results show that the Coriolis force effectively destroys the picture of cloud formation via TGI, rather than alleviate the problem of large angular momentum.

Subject headings: hydrodynamics — instabilities

[1]ARCSEC, Sejong University, Seoul 143-747, Korea

[2]Korea Astronomy & Space Science Institute, Daejeon 305-348, Korea

[3]Department of Astronomy & Space Science, Chungnam National University, Daejeon 305-764, Korea

[4]Department of Earth Sciences, Pusan National University, Pusan 609-735, Korea

1. Introduction

Thermal instability (TI) (Field 1965) is often invoked to explain a variety of physical phenomena in astrophysical environments: for instance, the multiple phases of interstellar gas (*e.g.,* Field *et al.* 1969; McKee & Ostriker 1977), the formation of globular clusters (*e.g.,* Fall & Rees 1985; Kang *et al.* 2000), cooling flows in clusters of galaxies (*e.g.,* Nulsen 1986), and the generation of turbulent flows in the interstellar medium (*e.g.,* Vázquez-Semadeni *et al.* 2000; Kritsuk & Norman 2002). Although the basic concept of TI as a local instability is rather simple and robust, the realistic situation is often more complex, involving effects such as magnetic field, turbulence, gravity, and rotation in case of galactic disks.

Recently the formation of structures via thermal-gravitational instability (TGI) in the protogalactic halo environment was studied using three-dimensional numerical simulations (Baek *et al.* 2005, hereafter Paper 1). The growth of density perturbations initially via TI and subsequently via gravitational infall and merging was followed up to $16-20$ cooling times in a periodic cubic box with size $L = 10$ kpc. The simulations showed that clumps emerge first on scales smaller than the cooling length as a result of non-linear behavior of TI. Those clumps grow through compression by background pressure, as well as through gravitational infall. Later during the gravitational merging stage, some clumps become gravitationally bound, virialized clouds with mass $M_c \gtrsim 6 \times 10^6 M_\odot$ and radius $R_c \approx 150 - 200$pc. However, these massive clouds acquire angular momentum through tidal torque and merging and have a large spin parameter $\langle \lambda_s \rangle \sim 0.3$. Hence removal of the angular momentum from theses clouds is critical, if they were to collapse further to form halo globular clusters such as in the model by Fall & Rees (1985).

In this paper we study the effects of rotation in protogalactic disk regions on the formation of clouds via TGI. Uniform rotation was included in the same numerical simulations as in Paper 1 to model protogalactic disk environment. In the next section we describe our models and numerical method. The simulation results are presented in §III. Summary follows in §IV.

2. Numerical Simulations

As in Paper 1, we consider a primordial gas of $T_h = 1.7 \times 10^6$K, which corresponds to the canonical temperature of an isothermal sphere with circular velocity $V_c = 220$ km s^{-1}, representing the hot phase of the gas in disk galaxies like the Milky Way. The fiducial value of the mean background density of hydrogen nuclei was chosen to be $n_h = 0.1$ cm^{-3}. For the primordial gas with an assumed ratio of He/H number densities of 1/10, the gas mass

density is given by $\rho_h = (2.34 \times 10^{-24}$ g) n_h. With $T_h = 1.7 \times 10^6$K and $n_h = 0.1$ cm^{-3}, the initial cooling time scale is $t_{\rm cool} = 2 \times 10^7$ yrs. On the other hand, the free-fall time scale, or the gravitational time scale, is $t_{\rm grav} = 1.4 \times 10^8$ yrs $\approx 7\ t_{\rm cool}$. Note that $t_{\rm cool} \propto n_h^{-1}$, while $t_{\rm grav} \propto n_h^{-1/2}$. So cooling, compared to gravitational processes, becomes relatively more important at higher densities and *vice versa*. The cooling length scale is defined as $l_{\rm cool} = c_h \cdot t_{\rm cool} = 4$ kpc, where $c_h = 198$ km s^{-1} is the sound speed.

To model the protogalactic disk environment, uniform rotation was incorporated by using a Cartesian coordinate system that rotates with angular velocity, $\Omega\hat{z}$. We chose as a fiducial value for the angular speed $\Omega_o = 27$ km s^{-1} kpc^{-1}, which corresponds to the Galactic rotation at the Solar circle ($R_o \approx 8.5$ kpc) (Feast & Whitelock 1997). A case with lower the angular speed, $\Omega_o/2$, was also considered for comparison. In the rotating frame, an additional Coriolis force term, $f_c = -2\Omega\hat{z} \times \mathbf{v}$, is added to the equation of motion. The simulation box was set to be cubic, with size $L = 10$ kpc $= 2.5 l_{\rm cool}$. The size was chosen to be large enough to accommodate a fair number of thermally unstable clouds of cooling length size, and so to obtain good statistics of cloud properties. Period boundary condition was imposed on the box, although it might not be the most natural choice for a disk-like geometry. We believe this particular choice of boundary condition would not affect the main conclusion regarding the role of rotation. Our periodic, cubic, simulation box represents a volume of disk region with significant rotation inside a protogalaxy.

To mimic density perturbations existed on a wide range of length scales inside the protogalaxies, the initial density field was drawn from random Gaussian fluctuations with predefined density power spectrum. The density power spectrum was assumed to be given by $P_k \propto k^n$ with $n = 0$ (white noise). In Paper 1 we showed that the properties of clouds, once formed, do not depend on initial fluctuation spectrum, although their spatial distribution is sensitive to the spectrum. Without *a priori* knowledge on initial fluctuations, a spectrum of constant power over all scales was chosen. The amplitude of the density power spectrum was fixed by the condition $\delta_{\rm rms} \equiv \langle \delta\rho^2 \rangle^{1/2} / \langle \rho \rangle = 0.2$. The initial temperature was set to be uniform, and the initial velocity was set to be zero everywhere.

The evolution of the gas from the initial perturbations was followed with 1) radiative cooling due to the primordial gas (Sutherland & Dopita 1993) down to $T = 10^4$ K, 2) background heating equal to the cooling of the initial, unperturbed background gas, and 3) self-gravity. The hydrodynamics was solved using an Eulerian hydrodynamic code based on the total variation diminishing scheme (Ryu *et al.* 1993) on a grid with 1024^3 cells (or 512^3 cells in the comparison run with $\Omega_o/2$). Simulations started at $t = 0$ and lasted up to $t_{\rm end} = 16 - 20 t_{\rm cool}$. Three simulations are presented in this paper, differing in angular speed. Model parameters are summarized in Table 1.

3. Results

We begin our discussion by comparing the Coriolis force to pressure force and gravity for the flows associated with the formation of clouds. First, the ratio of the Coriolis force to pressure force can be estimated roughly as

$$\frac{f_c}{f_p} \sim \frac{2\Omega_o v}{P_h/R_c\rho_h} \sim \frac{10\Omega_o R_c}{3c_h}, \tag{1}$$

where the typical flow speed is assumed to be similar to the sound speed, *i.e.,* $v \sim c_h$, and the adiabatic index of gas is $\gamma = 5/3$. Here R_c is the radius of typical clouds. Conservatively with $R_c \sim 100$ pc, the ratio is $f_c/f_p \sim 0.05$. So we expect that the effects of rotation are small, if not negligible, during the TI stage. The ratio of the Coriolis force to gravity can be written roughly as

$$\frac{f_c}{f_g} \sim \frac{2\Omega_o v R_c^2}{GM_c}. \tag{2}$$

Again with $v \sim c_h$, and conservatively with $M_c \sim 10^6$ $M_\odot$ and $R_c \sim 100$ pc, the ratio becomes $f_c/f_g \sim 25$. Hence during the gravitational infall and merging stages, the Coriolis force is expected to play a dominant dynamical role in our simulations with rotation.

The Coriolis force causes flows to be deflected at the right angle to the flow direction, hence it hinders spherical infall motions toward high density peaks, and generates circular motions in the plane perpendicular to the rotation axis. The Coriolis force also hinders the mergers of two clumps by drifting them to the opposite directions perpendicular to the line connecting two clouds, which leads to stretched worm-like structures. As a result, the formation of knot-like structures is suppressed and instead filamentary and sheet-like structures seem to appear.

Figure 1 shows the density power spectrum at different times. In the figure the dimensionless wavenumber is given as $k \equiv L/\lambda$. The power spectrum is presented in a way that $\int P_k dk = \langle \rho^2 \rangle$. During early stage $t \lesssim 6t_{\rm cool}$, the evolution of the density power spectrum looks similar in two models S1024 and R1024. It is because with $t_{\rm cool} < t_{\rm grav}$, initially the power grows mostly due to TI, and the Coriolis force has negligible effects. During $t \gtrsim 6t_{\rm cool}$, gravity controls the growth and so the two models evolve differently. In model S1024 the power continues to grow due to gravitational infall and merging over all scales. In model R1024, on the other hand, the Coriolis force suppresses the growth, more evidently on smaller scales. The comparison of the power spectrum of models R1024 ($\Omega = \Omega_o$) and RH512 ($\Omega = 0.5\Omega_o$) demonstrates the effects of different rotation speed. The figure shows that even with a half rotation speed the Coriolis force suppresses the growth of the power spectrum effectively.

To look at the shape and spatial distribution of formed structures, three-dimensional isodensity surfaces of a cubic region are shown in Figure 2. Initially clumps appear via TI in both models, as discussed in Paper 1 (see Figure 3 there). In model S1024, by $t = 8t_{\rm cool}$ the clumps have developed into distinct clouds with roughly spherical shapes. By $t = 12t_{\rm cool}$ some clouds have grown to be massive enough to become gravitationally bound, and by $t = 16t_{\rm cool}$ they have grown more massive. Those gravitationally bound clouds have the central density higher than 1000 times the mean background density. In model R1024, on the other hand, the initial clumps do not grow to distinct clouds. Instead loosely connected filamentary and sheet-like structures appear with the central density lower than 100 times the mean background density.

Although clouds are not distinctively defined in model R1024, we still identified clouds around high density peaks by the algorithm `clumpfind` described in Paper 1, and calculated their properties. The first row of Figure 3 shows the number of identified clouds, N_c, as a function of their mass, M_c. The mass function of the two models is almost identical at $t = 4t_{\rm cool}$. It is roughly Gaussian, since the initial density perturbations were drawn from a random Gaussian distribution. In model S1024, the mass function has evolved roughly into a log-normal distribution by $t = 8t_{\rm cool}$, which is a signature of nonlinear structure formation. At later stage the mass function extends to higher mass with a power-law distribution, as more massive clouds develop through gravitational merging. In model R1024, however, the mass distribution remains roughly Gaussian at $t = 8t_{\rm cool}$, and later it develops into a form, which is not well defined. This is another indication that the development of nonlinear structures has been severely altered by the Coriolis force.

The second row of Figure 3 shows the energy ratio of identified clouds, $\beta = 2(E_K + E_T)/|E_G|$. Here E_K is the kinetic energy defined in the center of mass of a given cloud, E_T is the thermal energy, and E_G is the gravitational energy. The parameter β tells us whether clouds are gravitationally bound ($\beta \lesssim 2$), and whether in virial equilibrium ($\beta \sim 1$). The figure shows that the virialized clouds with $M_c \gtrsim 6 \times 10^6$ M$_\odot$ have formed in model S1024. But in model R1024 the identified objects have $M_c \lesssim 10^6$ M$_\odot$, and none are gravitationally bound. We note that even in model RH512 with a half rotation speed, no gravitationally bound clouds were found.

The bottom row of Figure 3 shows the specific angular momentum of identified clouds. At $t = 4t_{\rm cool}$ the specific angular momentum is different in the two models, although other properties are similar. As mentioned earlier, clumps formed in the early stage gain angular momentum through the Coriolis effect, so j_c is higher in model R1024 than in model S1024. But during later stage angular momentum is acquired efficiently through torque and merging in model S1024, while it is not in model R1024. Hence for a given mass, j_c becomes higher

in model S1024 than in model R1024.

4. Summary

We study the effects of rotation in protogalactic disk regions on the formation of structures via TGI in the protogalactic environment. A simplified setting was considered, where a gas of primordial composition evolves from initial density perturbations in a uniformly rotating box. In Paper 1, we found that without rotation, virialized clouds of mass $M_c \gtrsim 6 \times 10^6$ $M_\odot$ can form as a result of TGI although they form with large angular momentum of spin parameter $\langle \lambda_s \rangle \sim 0.3$. In this paper we find that with rotation whose angular speed is comparable to that of the Galactic rotation at the Solar circle, $\Omega_o = 27$ km s^{-1} kpc^{-1}, the Coriolis force suppresses gravitational infall and merging and disperses the gas to filamentary and sheet-like structures. As a result, instead of massive virialized clouds formed in non-rotating models, clumps with $M_c \lesssim 10^6$ $M_\odot$, which are gravitationally unbound and often transient, are only found.

We conclude that the rotation in protogalactic disk regions has destructive effects on the formation of clouds, rather than alleviate the angular momentum problem discussed in Paper 1. The results in this paper and those in Paper 1 combined imply that it would be difficult for globular clusters to have formed via TGI in protogalaxies, and even less likely in rotating disk regions.

A few notes on our results: 1) Primordial gas is considered in this paper. But adding metal of order of 0.1 $Z_\odot$, which would enhance thermal processes, does not change the results, because it is the gravitational processes that are responsible for the formation of massive clouds but suppressed by the Coriolis force. We confirmed it with another simulation with metalicity of 0.1 $Z_\odot$, although we do not report the simulation in the paper. We point, however, that changing other parameters, for instance increasing the gas density by a factor of 10 in particular, would make differences. 2) The size of the simulation box we used, $L = 10$ kpc, along with periodic boundaries is too large to represent a protogalactic disk region. In order to check the effects of box size, we performed simulations in a smaller box of 2.5 kpc with 256^3 cells with and without rotation. Again although we do not report the simulation in details, the results confirmed that the formation of gravitationally bound objects is prohibited by the Coriolis force, regardless of the box size. 3) To be more realistic, differential rotation instead of uniform rotation needs to be investigated.

We thank the anonymous referee for clarifying comments. The work of C.H.B., H.K. and J.K. was supported by KOSEF through Astrophysical Research Center for the Structure

and Evolution of Cosmos (ARCSEC). The work of D.R. was supported by a Korea Research Foundation grant (KRF-2004-015-C00213). Simulations were run using Linux clusters at KASI and KISTI Supercomputing Center.

REFERENCES

Baek, C. H., Kang, H., Kim, J., & Ryu, D. 2005, ApJ, 630, 689 (Paper 1)

Fall, S. M., & Rees, M. J. 1985, ApJ, 298, 18

Feast, M., & Whitelock, P. 1997, MNRAS, 291, 683

Field, G. B. 1965, ApJ, 142, 531

Field, G. B., Goldsmith, D. W., & Habing, H. J. 1969, ApJ, 155, L149

Kang, H., Lake, G., & Ryu, D. 2000, Journal of Korean Astrophysical Society, 33, 111

Kritsuk, A. G., & Norman, M. L. 2002, ApJ, 569, L127

McKee, C. F., & Ostriker, J. P. 1977, ApJ, 218, 148

Nulsen, P. E. J. 1986, MNRAS. 221, 377

Ryu, D., Ostriker, J. P., Kang, H., & Cen, R. 1993, ApJ, 414, 1

Sutherland, R, S. & Dopita, M, A. 1993, ApJS, 88, 253

Vázquez-Semadeni, E., Gazol, A., & Scalo, J. 2000, ApJ, 540, 285

This preprint was prepared with the AAS LaTeX macros v5.2.

Table 1. Model Parameters for Simulations

Model	No. of Grid Zones	$t_{\rm end}$ $(t_{\rm cool})^{\rm a}$	$\Omega^{\rm b}$
S1024	1024^3	16	0.0
R1024	1024^3	16	Ω_o
RH512	512^3	20	$0.5\Omega_o$

[a] $t_{\rm cool} = 2 \times 10^7$ yrs

[b] $\Omega_0 = 27$ km s^{-1} kpc^{-1}.

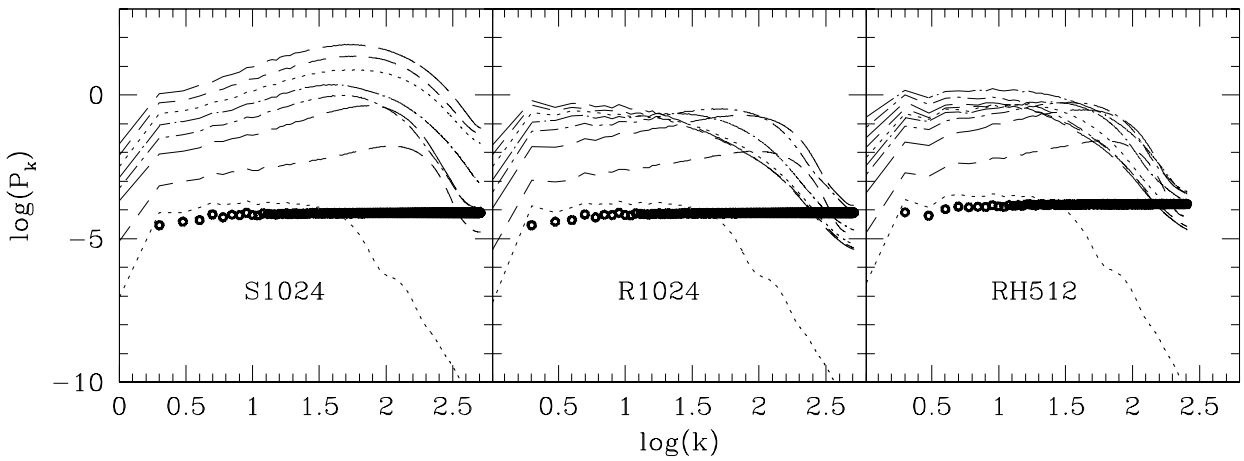

Fig. 1.— Evolution of the density power spectrum in models S1024, R1024, and RH512. Circles represent the initial power spectrum at $t = 0$. Lines show the power spectrum at 2 $t_{\rm cool}$, 4 $t_{\rm cool}$, 6 $t_{\rm cool}$, ..., 16 $t_{\rm cool}$ in models S1024 and R1024, and at 4 $t_{\rm cool}$, 6 $t_{\rm cool}$, ..., 20 $t_{\rm cool}$ in model RH512.

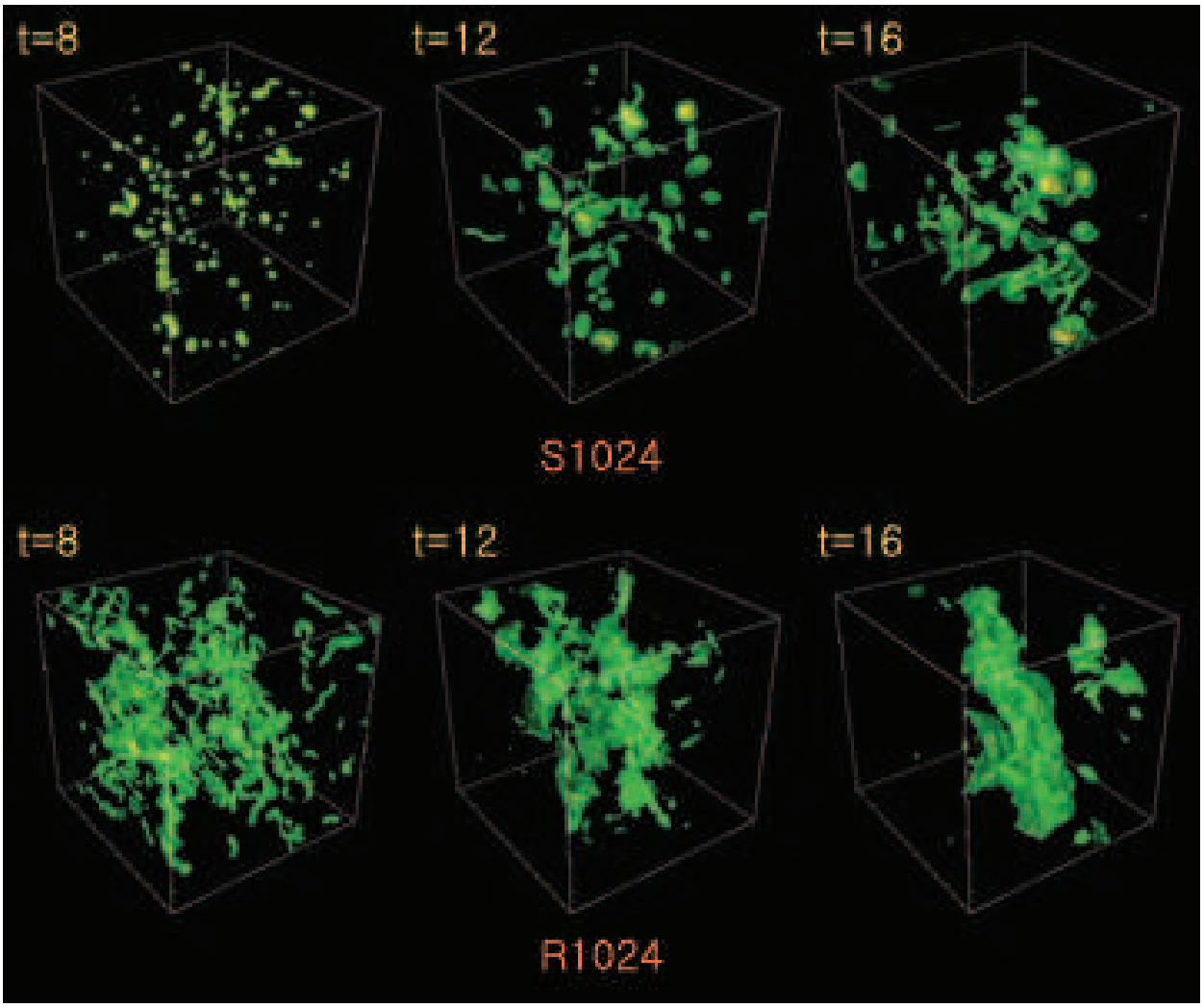

Fig. 2.— Isodensity surfaces inside a 2.5 kpc box of 256^3 grid zones, which is $(1/4)^3$ of the total simulation box, at 8 $t_{\rm cool}$, 12 $t_{\rm cool}$, and 16 $t_{\rm cool}$ in model S1024 (top panels), and in model R1024 (bottom panels). Green surfaces correspond to $10\rho_0$, yellow surfaces to $10^2\rho_0$, and red surfaces to $10^3\rho_0$. Here ρ_0 is the mean initial density. The box is oriented in such a way that the x, y, and $z-$axes are from near to far, from bottom to top, and from left to right, respectively. Rotation is along the $z-$axes in model R1024.

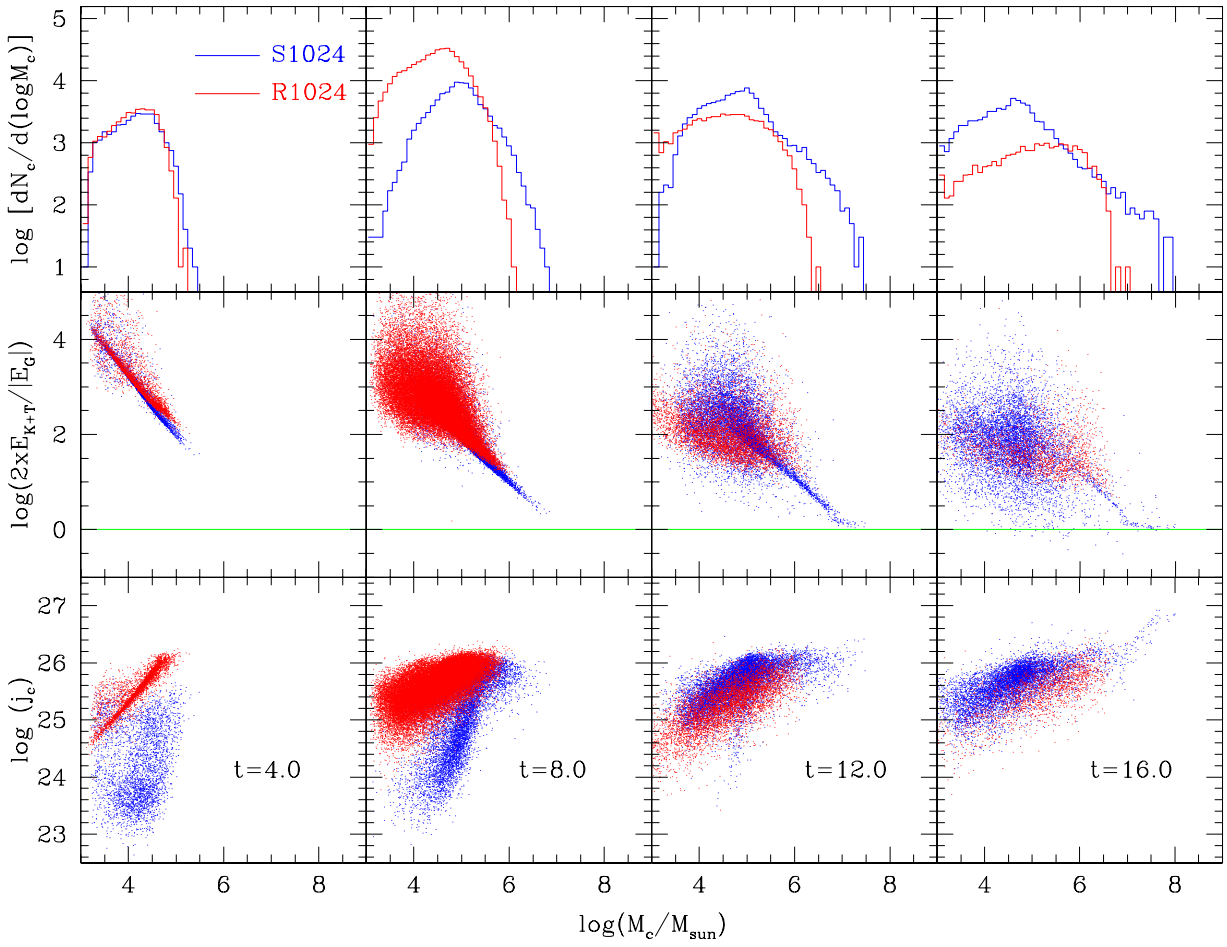

Fig. 3.— Differential number of clouds $dN_c/d(\log M_c)$, energy ratio, $2(E_T + E_K)/|E_G|$, and specific angular momentum j_c, as a function of cloud mass M_c, at four different times in models S1024 (blue color) and R1024 (red color). Here j_c is in cgs units.